Title

Coronary Plaque Characterization with T1-weighted MRI and Near-Infrared Spectroscopy to Predict Periprocedural Myocardial Injury.

Journal

Radiology: Cardiothoracic Imaging, 6(4)

Authors

Isodono, Koji
Matsumoto, Hidenari
Li, Debiao
et al.

Publication Date

2024-08-01

DOI

10.1148/ryct.230339

Peer reviewed

Radiology: Cardiothoracic Imaging

ORIGINAL RESEARCH

Coronary Plaque Characterization with T1-weighted MRI and Near-Infrared Spectroscopy to Predict Periprocedural Myocardial Injury

Koji Isodono, MD, PhD • Hidenari Matsumoto, MD, PhD* • Debiao Li, PhD • Piotr J. Slomka, PhD • Damini Dey, PhD • Sebastien Cadet, MS • Daisuke Irie, MD, PhD • Satoshi Higuchi, MD, PhD • Hiroki Tanisawa, MD, PhD • Motoki Nakazawa, MD • Yoshiaki Komori, MS • Hidefumi Ohya, MD • Ryoji Kitamura, MD, PhD • Tetsuichi Hondera, RT, MS • Ikumi Sato, RT • Hsu-Lei Lee, PhD • Anthony G. Christodoulou, PhD • Yibin Xie, PhD** •Toshiro Shinke, MD, PhD***

From the Departments of Cardiology (K.I., D.I., H.O., R.K.) and Radiological Technology (I.S.), Ijinkai Takeda General Hospital, Kyoto, Japan; Division of Cardiology (H.M., S.H., H.T., M.N., T.S.) and Department of Radiological Technology (T.H.), Showa University School of Medicine, 1-5-8 Hatanodai, Shinagawa-ku, Tokyo 142-8555, Japan; Biomedical Imaging Research Institute, Cedars-Sinai Medical Center, Los Angeles, Calif (D.L., P.J.S., D.D., S.C., H.L.L., A.G.C., Y.X.); and MR Research & Collaboration Department, Siemens Healthcare, Tokyo, Japan (Y.K.). Received October 22, 2023; revision requested December 26; revision received May 22, 2024; accepted July 13. **Address correspondence to** H.M. (email: *matsumoto.hidenari@med.showa-u.ac.jp*).

* K.I. and H.M. contributed equally to this work.

** Y.X. and T.S. are co–senior authors.

D.D. supported by grants from the National Institutes of Health and the National Heart, Lung, and Blood Institute (grant nos. 1R01HL14878701A1 and 1R01HL151266).

Conflicts of interest are listed at the end of this article.

Radiology: Cardiothoracic Imaging 2024; 6(4):e230339 • https://doi.org/10.1148/ryct.230339 • Content codes: VA MR

Purpose: To clarify the predominant causative plaque constituent for periprocedural myocardial injury (PMI) following percutaneous coronary intervention: *(a)* erythrocyte-derived materials, indicated by a high plaque-to-myocardium signal intensity ratio (PMR) at coronary atherosclerosis T1-weighted characterization (CATCH) MRI, or *(b)* lipids, represented by a high maximum 4-mm lipid core burden index ($maxLCBI_{4\ mm}$) at near-infrared spectroscopy intravascular US (NIRS-IVUS).

Materials and Methods: This retrospective study included consecutive patients who underwent CATCH MRI before elective NIRS-IVUS–guided percutaneous coronary intervention at two facilities. PMI was defined as post–percutaneous coronary intervention troponin T values greater than five times the upper reference limit. Multivariable analysis was performed to identify predictors of PMI. Finally, the predictive capabilities of MRI, NIRS-IVUS, and their combination were compared.

Results: A total of 103 lesions from 103 patients (median age, 72 years [IQR, 64–78]; 78 male patients) were included. PMI occurred in 36 lesions. In multivariable analysis, PMR emerged as the strongest predictor ($P = .001$), whereas $maxLCBI_{4\ mm}$ was not a significant predictor ($P = .07$). When PMR was excluded from the analysis, $maxLCBI_{4\ mm}$ emerged as the sole independent predictor ($P = .02$). The combination of MRI and NIRS-IVUS yielded the largest area under the receiver operating curve (0.86 [95% CI: 0.64, 0.83]), surpassing that of NIRS-IVUS alone (0.75 [95% CI: 0.64, 0.83]; $P = .02$) or MRI alone (0.80 [95% CI: 0.68, 0.88]; $P = .30$).

Conclusion: Erythrocyte-derived materials in plaques, represented by a high PMR at CATCH MRI, were strongly associated with PMI independent of lipids. MRI may play a crucial role in predicting PMI by offering unique pathologic insights into plaques, distinct from those provided by NIRS.

Supplemental material is available for this article.

Periprocedural myocardial injury (PMI) following elective percutaneous coronary intervention (PCI) remains a major concern, with a prevalence ranging from 10% to 40% (1–4). PMI is primarily attributed to distal embolization of fragile atheromatous or thrombotic materials resulting from balloon dilatation or stent implantation (4). PMI is related to adverse clinical outcomes and prolonged hospital stays requiring additional medical costs (1,3). Therefore, it is crucial to identify lesions at high risk of distal embolization, aiding in the proper implementation of preventive measures to alleviate the occurrence and severity of PMI, including the use of distal protection devices (5). Consequently, many studies have focused on identifying imaging features associated with distal embolization (6).

It is widely recognized that a large lipid core is a histopathologic hallmark of plaques that cause PMI (6–8). Near-infrared spectroscopy (NIRS) imaging enables the specific identification of lipid components within atherosclerotic plaques and provides a unique quantitative measure, namely the maximum 4-mm lipid core burden index ($maxLCBI_{4\ mm}$) (9). Several studies have demonstrated the predictive value of NIRS for PMI (7,10–13). Nevertheless, certain cases of PMI have been observed in lesions with relatively low $maxLCBI_{4\ mm}$ values (10–12,14).

Erythrocytes also have a crucial role in the development of PMI (4,15–17). MRI is ideal for detecting erythrocyte-derived materials (18,19). At noncontrast T1-weighted MRI, erythrocytes containing methemoglobin with a

Abbreviations

CATCH = coronary atherosclerosis T1-weighted characterization, cTnT = cardiac troponin T, IVUS = intravascular US, maxLCBI$_{4\,mm}$ = maximum 4-mm lipid core burden index, NIRS = near-infrared spectroscopy, PCI = percutaneous coronary intervention, PMI = periprocedural myocardial injury, PMR = plaque-to-myocardium signal intensity ratio

Summary

This study demonstrates that T1-weighted MRI plays a crucial role in helping to predict periprocedural myocardial injury by offering unique pathologic insights into plaques from a different perspective than lipid assessment with near-infrared spectroscopy.

Key Points

- A high plaque-to-myocardium signal intensity ratio at T1-weighted MRI, indicative of erythrocyte-derived materials within coronary plaques, emerged as the strongest predictor of periprocedural myocardial injury in the multivariable analysis including parameters from near-infrared spectroscopy intravascular US (NIRS-IVUS) and MRI (odds ratio, 1.35 per 0.1 increase in plaque-to-myocardium signal intensity ratio value; $P < .001$).
- Receiver operating characteristic curve analysis revealed that the combination of NIRS-IVUS and MRI provided the best predictive capability, with an area under the receiver operating curve of 0.86, surpassing that of NIRS-IVUS alone (0.75; $P = .02$).

Keywords

Coronary Plaque, Periprocedural Myocardial Injury, MRI, Near-Infrared Spectroscopy Intravascular US

short T1 relaxation time exhibit high signal intensity (20). The plaque-to-myocardium signal intensity ratio (PMR) at T1-weighted MRI has been demonstrated to be a powerful predictor of PMI (15–17). The coronary atherosclerosis T1-weighted characterization (CATCH) with integrated anatomic reference technique allows for reliable assessment of PMR by simultaneously acquiring inherently coregistered dark-blood plaque and bright-blood coronary artery images (19,21).

Thus far, little is known about the predominant causative plaque constituent for PMI: lipids, erythrocytes, or both. This study aimed to address this question by comparing the predictive capabilities of CATCH MRI and NIRS–intravascular US (IVUS) for PMI.

Materials and Methods

This study is a retrospective analysis of an ongoing prospective observational study that was approved by the institutional review board to assess the feasibility of CATCH MRI for predicting PMI. All patients provided written informed consent for the research CATCH MRI scan. The institutional review board approved this retrospective Health Insurance Portability and Accessibility Act–compliant study. The authors who were not employees of Siemens had complete control of data collection and analysis.

Study Patients

Inclusion and exclusion criteria are detailed in Appendix S1. We reviewed 156 lesions from 156 patients who underwent CATCH MRI followed by elective stent implantation with NIRS-IVUS guidance within 3 months at two facilities. In a prior study, we reported on 63 patients included in the current study. The prior report evaluated the morphology of high-intensity plaques at T1-weighted MRI (19).

Procedures

CATCH MRI.—MRI was performed on commercially available scanners (1.5-T Magnetom Avanto or 3.0-T Magnetom Skyra; Siemens Healthcare). The CATCH sequence was based on a three-dimensional, prospective electrocardiographically gated, inversion recovery–prepared spoiled gradient-echo sequence (21). Noncontrast CATCH MRI was conducted as previously described (details in Appendix S1) (19). This technique acquired dark-blood T1-weighted plaque and bright-blood anatomic reference images simultaneously by applying the inversion recovery pulse in an interleaved fashion, allowing two spatially matched sets of images (21).

NIRS-IVUS–guided PCI and Measurement of Cardiac Troponin T.—NIRS-IVUS–guided PCI was performed using contemporary drug-eluting stents in a standard fashion as described elsewhere (14,22). Preintervention NIRS-IVUS images were obtained with a commercially available catheter and imaging system (Nipro). A distal protection device was not used in this study sample.

High-sensitivity cardiac troponin T (cTnT) values were measured before and 12–24 hours after PCI (2,4,10,11,14,23). PMI was defined as post-PCI cTnT levels greater than five times the upper reference limit (70 ng/L) (4). Lesions with PMI were assigned to the PMI group, and the others were assigned to the non-PMI group. The magnitude of cTnT elevation was calculated as the difference between post-PCI cTnT levels and pre-PCI cTnT levels.

Image Analysis

Offline image analyses were performed by the consensus of experienced observers. NIRS-IVUS and MR images were independently analyzed by separate observers who were unaware of other imaging findings and clinical data.

CATCH MRI.—CATCH MR images were analyzed using dedicated software (FusionQuant version 1.21, Cedars-Sinai Medical Center) (23) by two observers (H.M. and M.N., with 16 and 2 years of experience with cardiac MRI, respectively). Details are provided in Figure 1 and Appendix S1. Briefly, once the lumen centerline within the treated segment on the bright-blood coronary artery images was tracked, the software automatically determined the highest signal intensity on the inherently coregistered dark-blood plaque images along the centerline that encompassed the coronary artery and its immediate surroundings (typically a 3-mm radius).

PMR was calculated as the highest plaque signal intensity divided by the mean signal intensity of the nearby left ventricular myocardium (16,19,23,24). A lesion with a PMR value of 1.4 or greater was categorized as a high-intensity plaque (19,24).

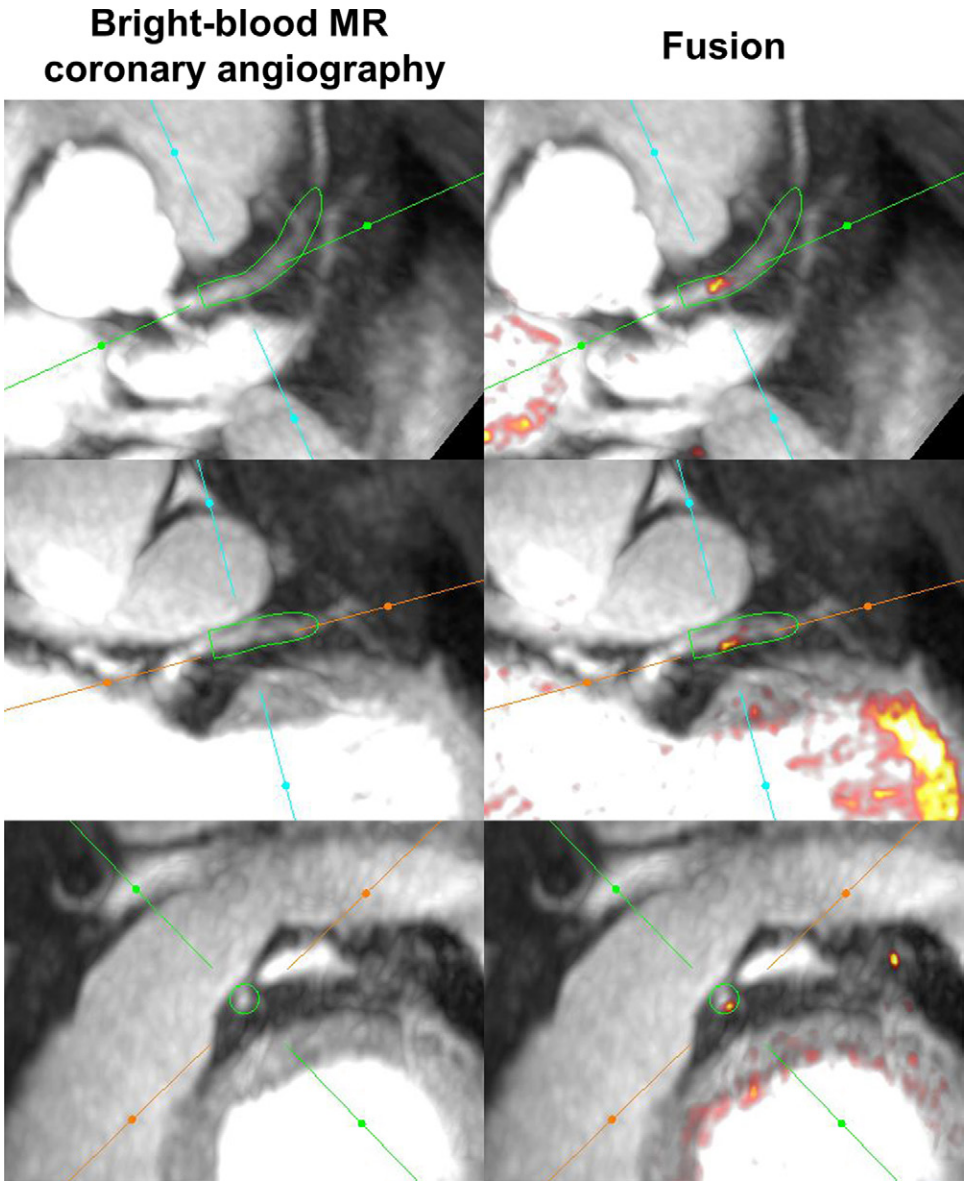

Figure 1: Semiautomated assessment of high-intensity plaque. Multiplanar reformatted bright-blood MR images of the left anterior descending artery are shown. After tracking the lumen centerline within the treated segment on the bright-blood coronary artery images, the software automatically generated tubular three-dimensional volumes of interest encompassing the coronary artery and its immediate surroundings (left panel). Color-coded overlays on the right panel correspond to the signal intensity on inherently coregistered dark-blood T1-weighted images. Within the designated volumes of interest, the software automatically computed the highest signal intensity. Whole-heart coronary atherosclerosis T1-weighted characterization MR images are available in the Movie.

NIRS-IVUS.—NIRS-IVUS data were analyzed using dedicated software (echoPlaque version 4.3; INDEC Medical Systems) as previously reported (details in Appendix S1) (14,19,22,25) by two observers, with 19 years (K.I.) and 12 years (D.I.) of experience in intracoronary imaging. The lipid core burden index represented the fraction of pixels that exhibit a high probability (>0.6) of containing a lipid core within a specified segment multiplied by 1000 (9). MaxLCBI$_{4\ mm}$ was defined as the maximum value of the lipid core burden index observed within any 4-mm long segment (9). A lipid-rich plaque was defined as maxLCBI$_{4\ mm}$ greater than 400 (19).

Statistical Analysis

Continuous variables are reported as medians with IQRs. Categorical variables are presented as frequencies with corresponding percentages. Between-group comparisons of quantitative variables were made with either the unpaired sample *t* test or Mann-Whitney *U* test, and categorical variables were compared using the χ^2 test or Fisher exact test, as appropriate. When comparing three subgroups, the Kruskal–Wallis test was employed for continuous variables, and Fisher exact test was used for categorical variables. Spearman rank correlation coefficient was used to assess the correlations between PMR and maxLCBI$_{4\ mm}$.

Univariable and multivariable logistic regression analyses were used to identify predictors of PMI. MaxLCBI$_{4\ mm}$, PMR, and factors with a univariable association of $P < .10$ were included as explanatory variables in the multivariable model. In this study, two multivariable models were evaluated: Model 1 consisted of NIRS-IVUS–derived variables, and model 2 included NIRS-IVUS–derived variables and PMR. Receiver operating characteristic curve analysis was applied to determine the predictive performance of NIRS-IVUS alone, CATCH MRI alone, and their combination. The DeLong test was used to evaluate the differences in the area under the receiver operating characteristic curve (26). *P* values were adjusted using the Bonferroni correction method for multiple comparisons. The cutoff value was determined as the point that maximized the Youden index.

Statistical analyses were performed using JMP Pro (version 16.0.0.; SAS Institute). *P* values less than .05 were considered to indicate statistical significance.

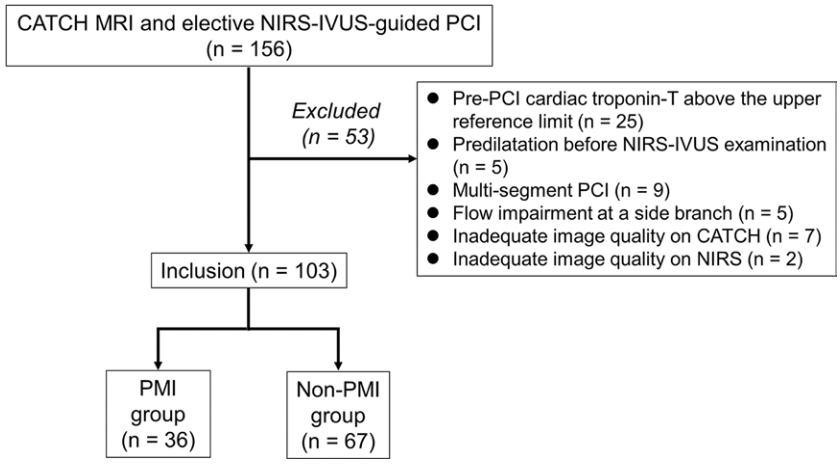

Figure 2: Flowchart of study selection. CATCH = coronary atherosclerosis T1-weighted characterization, NIRS-IVUS = near-infrared spectroscopy intravascular US, PCI = percutaneous coronary intervention, PMI = periprocedual myocardial injury.

Results

Baseline Characteristics and Procedural Findings

Figure 2 shows a flowchart outlining the inclusion of lesions. A total of 53 lesions were excluded from the study for the following reasons: *(a)* pre-PCI cTnT values above the upper reference limit of 14 ng/L ($n = 25$), *(b)* predilatation before NIRS-IVUS examination ($n = 5$), *(c)* stent implantation for separated segments or two or more vessels in a single procedure ($n = 9$), *(d)* flow impairment observed at any visible side branch with a thrombolysis in myocardial infarction flow grade of less than or equal to 2 ($n = 5$), and *(e)* inadequate image quality observed at CATCH MRI ($n = 7$) or NIRS-IVUS ($n = 2$). In the final analysis, 103 lesions from 103 patients were included. The median age of patients was 72 years (IQR, 68–78 years); 78 patients (76%) were male and 25 (24%) were female.

Out of the 103 lesions, 36 (35%) were categorized into the PMI group, whereas 67 (65%) were classified into the non-PMI group. The median cTnT value elevation was 13 ng/L (IQR, 7–26 ng/L) for the non-PMI group and 114 ng/L (IQR, 91–208 ng/L) for the PMI group. There was no evidence of a difference in the time interval between MRI and PCI between groups (6 days [IQR, 1–30 days] in the non-PMI group vs 3 days [IQR, 1–30 days] in the PMI group; $P = .78$). Table 1 compares patient, angiographic, and procedural characteristics between the non-PMI and PMI groups. The incidence of thrombolysis in myocardial infarction flow grade less than or equal to 2 during the PCI procedure was higher in the PMI group (17% [six of 36] vs 2% [three of 67]; $P = .02$). The PMI group more frequently required a prolonged hospital stay beyond what was initially planned (14% [five of 36] vs 1% [one of 67]; $P = .02$).

NIRS-IVUS and CATCH MRI Findings

The median maxLCBI$_{4\ mm}$ was 446 (IQR, 206–630), with 59 lesions categorized as having lipid-rich plaque at NIRS (maxLCBI$_{4\ mm}$ > 400). The median PMR was 1.23 (IQR, 1.10–1.45), and 36 lesions were characterized as having high-intensity plaque based on CATCH MRI findings (PMR ≥ 1.4).

Table 2 presents a comparison of NIRS-IVUS and CATCH findings between the PMI and non-PMI groups. In terms of gray-scale IVUS parameters, the PMI group exhibited a longer lesion length (31 mm [IQR, 23–40 mm] vs 23 mm [IQR, 17–32 mm]; $P = .003$), a smaller minimum lumen area (1.92 mm^2 [IQR, 1.62–2.49 mm^2] vs 2.53 mm^2 [IQR, 1.97–3.64 mm^2]; $P < .001$), and a larger plaque burden (82.8% [IQR, 75.8%–86.7%] vs 77.6% [IQR, 71.7%–83.6%]; $P = .02$) than the non-PMI group. MaxLCBI$_{4\ mm}$ was higher in the PMI group than in the non-PMI group (589 [IQR, 400–767] vs 376 [IQR, 136–514]; $P < .001$). Lipid-rich plaque was observed in 75% (27 of 36) of the PMI group and 48% (32 of 67) of the non-PMI group ($P < .001$). At CATCH MRI, PMR was higher in the PMI group than in the non-PMI group (1.46 [IQR, 1.28–1.89] vs 1.16 [IQR, 1.08–1.28]; $P < .001$). Among the lesions in the PMI group, 58% (21 of 36) were categorized as high-intensity plaque, whereas in the non-PMI group, 12% (eight of 67) were classified as such ($P < .001$).

Predictors of PMI

Based on the results of the univariable analysis assessing the association with PMI (Table S1), the following NIRS-IVUS–derived parameters were included in the multivariable analyses: *(a)* maxLCBI$_{4\ mm}$ ($P < .001$), *(b)* minimum lumen area ($P = .004$), *(c)* plaque burden ($P = .02$), and *(d)* lesion length ($P = .02$). Table 3 presents the results of the multivariable analyses. In model 1, which incorporates NIRS-IVUS–derived parameters, maxLCBI$_{4\ mm}$ emerged as the sole independent predictor (odds ratio, 1.27 per 100 increase [95% CI: 1.03, 1.57]; χ^2, 5.18; $P = .02$). Model 2, which includes PMR in addition to the NIRS-IVUS–derived parameters, identified PMR (odds ratio, 1.35 per 0.1 increase [95% CI: 1.16, 1.67]; χ^2, 10.69; $P < .001$) and minimum lumen

Table 1: Patient, Angiographic, and Procedural Characteristics

Parameter	All (n = 103)	Non-PMI Group (n = 67)	PMI Group (n = 36)	P Value
Age (y)	72 (64–78)	70 (63–78)	74 (66–79)	.31
Male, female (n)	78, 25	49, 18	29, 7	.40
Body mass index (kg/m^2)	23.7 (21.8–26.5)	23.9 (22.2–27.2)	22.9 (20.7–25.2)	.13
Hypertension	71 (69)	45 (67)	26 (72)	.57
Dyslipidemia	87 (84)	56 (84)	31 (86)	.74
Diabetes mellitus	38 (37)	27 (40)	11 (31)	.33
Current smoking	18 (17)	9 (13)	9 (25)	.14
Prior myocardial infarction	6 (6)	4 (6)	2 (6)	>.99
Prior revascularization	22 (21)	15 (22)	7 (19)	.73
LDL cholesterol (mg/dL)	86 (63–105)	87 (60–104)	78 (63–107)	.59
HDL cholesterol (mg/dL)	50 (42–61)	49 (42–60)	51 (42–64)	.63
Triglycerides (mg/dL)	116 (83–166)	121 (87–166)	106 (79–165)	.34
Glycated hemoglobin (%)	6.1 (5.7–6.7)	6.1 (5.8–6.8)	6.1 (5.6–6.7)	.25
eGFR (mL/min)	68.8 (58.7–81.4)	68.9 (59.1–81.4)	66.4 (51.6–81.6)	.90
Medications				
Statin	94 (91)	63 (94)	31 (86)	.27
Ezetimibe	42 (71)	29 (43)	13 (36)	.48
ß-Blocker	36 (35)	10 (28)	26 (39)	.26
Renin-angiotensin system blocker	44 (43)	29 (43)	15 (42)	.87
Calcium channel blocker	41 (40)	25 (37)	16 (44)	.48
Insulin	5 (5)	3 (4)	2 (6)	>.99
P2Y12 inhibitor (clopidogrel, prasugrel)	41, 62	25, 42	16, 20	.48
Cardiac troponin T				
Pre-PCI (ng/L)	8 (6–11)	8 (5–11)	9 (6–11)	.48
Post-PCI (ng/L)	36 (18–104)	22 (15–35)	120 (99–218)	NA
Post-PCI to pre-PCI (ng/L)	28 (11–95)	13 (7–26)	114 (91–208)	NA
Angiographic findings				
Target vessel (LAD, LCX, RCA)	66, 15, 22	41, 10, 16	25, 5, 6	.66
Proximal lesion	37 (36)	27 (40)	10 (28)	.21
Type B2/C lesion	78 (76)	48 (72)	30 (83)	.19
No. of patients with 1, 2, or 3 diseased vessels	73, 27, 3	50, 15, 2	23, 12, 1	.44
SYNTAX score	8 (6–12)	8 (6–11)	9 (8–13)	.13
Pre-PCI TIMI flow grade ≤ 2	11 (11)	7 (10)	4 (11)	>.99
Post-PCI TIMI flow grade ≤ 2	2 (2)	0 (0)	2 (6)	.12
TIMI flow grade ≤ 2 during the procedure	8 (8)	2 (3)	6 (17)	.02
Procedural characteristics				
Maximum stent diameter (mm)	3.00 (2.75–3.50)	3.00 (2.75–3.50)	3.00 (2.81–3.50)	.81
No. of stents	1 (1–1)	1 (1–1)	1 (1–2)	.07
Maximum balloon size (mm)	3.50 (3.23–3.50)	3.50 (3.23–3.50)	3.50 (3.06–3.94)	.42
Postdilatation with an upsized balloon	58 (56)	37 (55)	21 (58)	.76
Direct stent placement	21 (20)	13 (19)	8 (22)	.74

Note.—Unless otherwise noted, data are expressed as medians with IQRs in parentheses or values with percentages in parentheses. eGFR = estimated glomerular filtration rate, HDL = high-density lipoprotein, LAD = left anterior descending coronary artery, LCX = left circumflex coronary artery, LDL = low-density lipoprotein, NA = not applicable, PCI = percutaneous coronary intervention, PMI = periprocedual myocardial injury, RCA = right coronary artery, TIMI = thrombolysis in myocardial infarction.

area (odds ratio, 0.37 per 1 mm^2 increase [95% CI: 0.15, 0.89]; χ^2, 4.95; P = .03) as independent predictors. The association between maxLCBI$_{4\,mm}$ and PMI did not reach statistical significance (odds ratio, 1.25 per 100 increase [95% CI: 0.99, 1.58]; χ^2, 3.38; P = .07). Based on the receiver operating characteristic curve analysis, the optimal cutoff value for predicting PMI was 474 for maxLCBI$_{4\,mm}$ and 1.33 for the PMR.

According to the results of the multivariable analyses, we developed three prediction models: *(a)* NIRS-IVUS alone, incorporating maxLCBI$_{4\,mm}$ and minimum lumen area; *(b)*

Table 2: Near-Infrared Spectroscopy–Intravascular US and MRI Findings

Parameter	All (n = 103)	Non-PMI Group (n = 67)	PMI Group (n = 36)	P Value
Gray-scale IVUS				
Lesion length (mm)	24 (18–38)	23 (17–32)	31 (23–40)	.003
External elastic membrane area (mm^2)	12.4 (9.6–16.3)	12.7 (9.6–16.4)	12.3 (8.9–16.0)	.76
Minimum lumen area (mm^2)	2.23 (1.79–3.32)	2.53 (1.97–3.64)	1.92 (1.62–2.49)	<.001
Plaque burden (%)	80.3 (72.8–85.0)	77.6 (71.7–83.6)	82.8 (75.8–86.7)	.02
Remodeling index	0.91 (0.76–1.05)	0.92 (0.73–1.06)	0.89 (0.78–1.05)	.92
Calcification				
Presence	88 (85)	55 (82)	33 (92)	.19
Spotty calcification	45 (44)	30 (45)	15 (42)	.76
NIRS				
Lipid core burden index	166 (80–261)	126 (40–207)	242 (137–307)	<.001
$MaxLCBI_{4\ mm}$	446 (206–630)	376 (136–514)	589 (400–767)	<.001
Lipid-rich plaque	59 (57)	32 (48)	27 (75)	.008
MRI				
Plaque-to-myocardium signal intensity ratio	1.23 (1.10–1.45)	1.16 (1.08–1.28)	1.46 (1.28–1.89)	<.001
High-intensity plaque	29 (28)	8 (12)	21 (58)	<.001

Note.—Data are expressed as medians with IQRs in parentheses or values with percentages in parentheses. Lipid-rich plaque was defined as maximum 4-mm lipid core burden index values ($maxLCBI_{4\ mm}$) greater than 400, and high-intensity plaque was identified as a plaque-to-myocardium signal intensity ratio value greater than or equal to 1.4. IVUS = intravascular US, NIRS = near-infrared spectroscopy, PMI = periprocedual myocardial injury.

Table 3: Predictors of Periprocedual Myocardial Injury at Multivariable Analysis

	Model 1			Model 2		
Parameter	Odds Ratio	Chi-squared	P Value	Odds Ratio	Chi-squared	P Value
$MaxLCBI_{4\ mm}$ (per 100 increase)	1.27 (1.03–1.57)	5.18	.02	1.25 (0.99–1.58)	3.38	.07
Minimum lumen area (per 1 mm^2 increase)	0.68 (0.38–1.25)	1.53	.22	0.37 (0.15–0.89)	4.95	.03
Plaque burden (per 1% increase)	1.03 (0.97–1.09)	0.97	.33	0.98 (0.92–1.06)	0.19	.66
Lesion length (per 1 mm increase)	1.02 (0.98–1.06)	0.74	.39	1.02 (0.97–1.06)	0.54	.46
PMR (per 0.1 increase)	NA	NA	NA	1.35 (1.16–1.67)	10.69	.001

Note.—Data are expressed as values or values with 95% CI in parentheses. $maxLCBI_{4\ mm}$ = maximum 4-mm lipid core burden index, NA = not applicable, PMR = plaque-to-myocardium signal intensity ratio.

CATCH MRI alone, using PMR; and *(c)* the integration of NIRS-IVUS and CATCH MRI, combining $maxLCBI_{4\ mm}$, minimum lumen area, and PMR. As displayed in Figure 3, the largest area under the receiver operating characteristic curve was achieved by NIRS-IVUS and CATCH MRI: 0.86 (95% CI: 0.64, 0.83). In comparison, the area under the receiver operating characteristic curve was 0.75 (95% CI: 0.64, 0.83; P = .02) for NIRS-IVUS alone and 0.80 (95% CI: 0.68, 0.88; P = .30) for CATCH MRI alone.

Lipid-rich Plaque at NIRS and High-Intensity Plaque at CATCH MRI

Figure 4 displays the scatterplot of $maxLCBI_{4\ mm}$ and PMR. The correlation of the two indexes was weak (ρ = 0.24; P =

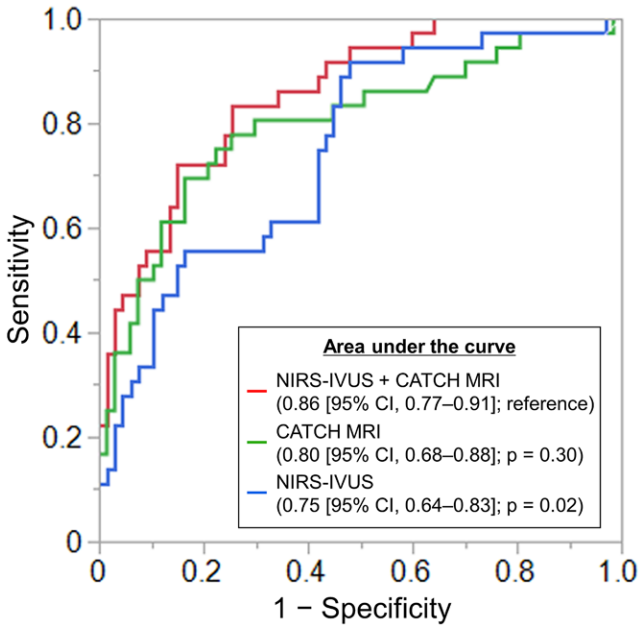

Figure 3: Predictive performance of near-infrared spectroscopy (NIRS), MRI, and their combination for periprocedural myocardial injury. Receiver operating characteristic curves were generated to assess the predictive capabilities of coronary atherosclerosis T1-weighted characterization (CATCH) MRI, NIRS–intravascular US (IVUS), and their combination. *P* values were adjusted using Bonferroni correction to account for multiple comparisons.

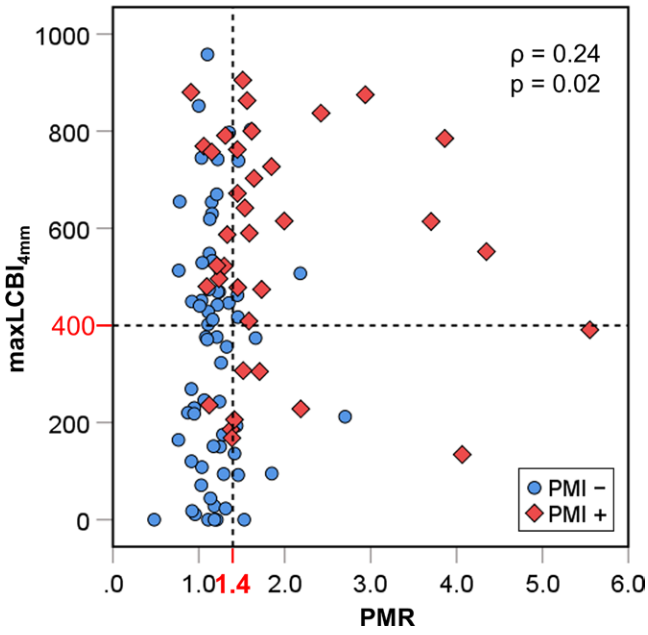

Figure 4: Scatterplot of plaque-to-myocardium signal intensity ratio (PMR) and maximum 4-mm lipid core burden index (maxLCBI$_{4\,mm}$). PMI = periprocedural myocardial injury.

.02). The agreement between lipid-rich plaque at NIRS and high-intensity plaque at CATCH MRI was slight (κ = 0.09 [95% CI: −0.07 to 0.25]; *P* = .29). Categorical disagreement was observed in 49% (50 of 103) of the lesions, with 39% (40 of 103) classified as lipid-rich plaque alone and 10% (10 of 103) categorized as high-intensity plaque alone.

Lesions were divided into three groups based on the presence of lipid-rich plaque and high-intensity plaque: *(a)* lesions with both types of plaque, *(b)* lesions with either type of plaque alone, and *(c)* lesions with neither type of plaque. As shown in Figure 5A, the incidence of PMI was highest in lesions with both lipid-rich plaque and high-intensity plaque (84% [16 of 19]), followed by lesions with either type of plaque alone (32% [16 of 50]) and lesions with neither type of plaque (12% [four of 34]) (*P* < .001 for all group comparisons). Similarly, lesions with both lipid-rich plaque and high-intensity plaque exhibited the highest cTnT value elevation, followed by lesions with either type of plaque alone and lesions with neither type of plaque (Fig 5B) (*P* < .001 for all group comparisons). Figure 6 illustrates examples of a lesion with lipid-rich plaque and high-intensity plaque associated with PMI.

Discussion

Our evaluation of CATCH MRI and NIRS-IVUS in patients undergoing elective stent implantation revealed that a high PMR value at CATCH MRI, indicative of erythrocyte-derived materials within coronary plaques, is the strongest predictor of PMI, independent of lipid components represented by a high maxLCBI$_{4\,mm}$ at NIRS.

In line with earlier reports (7,10–12), maxLCBI$_{4\,mm}$ at NIRS was found to be predictive of PMI. However, it is noteworthy that 25% of PMI in the current study arose from non-lipid-rich plaques. The distribution of maxLCBI$_{4\,mm}$ values exhibited considerable overlap between the PMI and non-PMI groups in the present study (IQR, 400–767 vs 136–514) as well as in the previous study with the largest sample size (IQR, 382–639 vs 162–553) (12). These findings suggest that the risk of distal embolization may not be solely attributed to the presence of lipids within the plaque, but also involves other plaque components.

T1-weighted MRI helps provide unique insights into the pathophysiology of coronary atherosclerotic plaques from a different perspective than lipids (19). Consistent with earlier research on the carotid artery (18), histopathologic studies in the coronary artery have confirmed that erythrocyte-derived materials, rather than lipids, are the predominant substrate of coronary high-intensity plaque at noncontrast T1-weighted MRI (27,28). To our knowledge, this study is the first to provide evidence that PMR as measured with T1-weighted MRI is the strongest predictor of PMI independently of maxLCBI$_{4\,mm}$ obtained with NIRS. The result suggests that erythrocyte-derived materials within plaques may be the predominant causative plaque component. Our findings highlight the crucial role of T1-weighted MRI in coronary plaque characterization.

Various noninvasive and intravascular imaging modalities have been proposed to predict PMI (6). However, using specific imaging features from invasive imaging modalities, such as thin-cap fibroatheroma at optical coherence tomography and attenuated plaque and echolucent plaque at gray-scale IVUS, may not be feasible in routine clinical settings. Image analysis during the PCI procedure necessitates specialized expertise and is susceptible to interobserver variability. In contrast, NIRS offers an automated real-time quantitative analysis of lipid burden, eliminating the need for interpretation by readers (9). As noted above, T1-weighted MRI helps provide information that

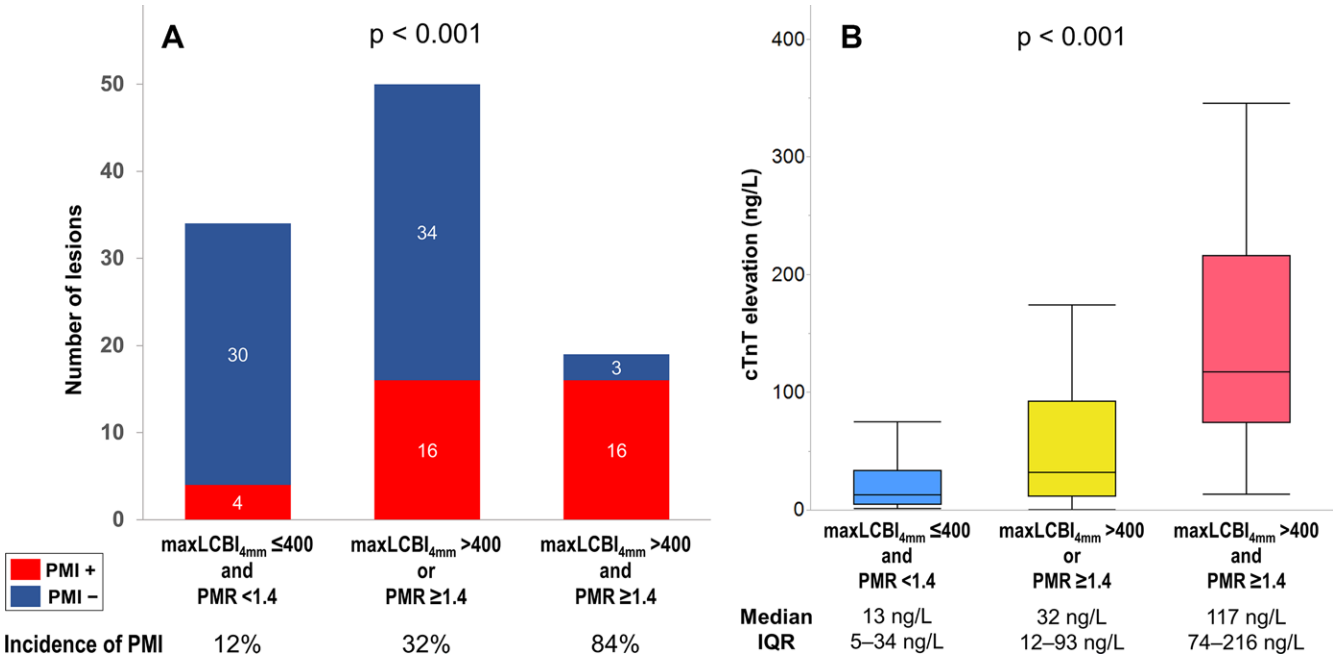

Figure 5: Graphs show the **(A)** incidence of periprocedual myocardial injury (PMI) and **(B)** cardiac troponin T (cTnT) value elevation according to the presence of lipid-rich plaque and high-intensity plaque. Lipid-rich plaque was defined as maximum 4-mm lipid core burden index ($maxLCBI_{4\ mm}$) value greater than 400 at near-infrared spectroscopy, and high-intensity plaque was defined as plaque-to-myocardium signal intensity ratio (PMR) greater than or equal to 1.4 at MRI. cTnT value elevation was calculated as the difference between post-PCI cTnT levels and pre-PCI cTnT levels.

is distinct from NIRS (19,27–29). Conventional MR pulse sequence and analysis methods typically require experienced readers and may be prone to variability (30). Our semiautomated analysis of CATCH images, for which spatial alignment between anatomic reference and plaque images is guaranteed, alleviates the need for reader expertise and reduces variability. Consequently, the combination of NIRS and CATCH MRI would be an ideal approach for predicting PMI. Conducting MRI for all patients before PCI is not feasible in clinical practice. Given that coronary CT angiography is recommended as the preferred first-line test for managing coronary artery disease (31–33), it is crucial to identify the specific subset of patients who should undergo MRI based on their CT findings. Further investigation is warranted to determine how MRI should be implemented for patients undergoing elective PCI.

A randomized study failed to demonstrate the benefit of using a distal protection device for lesions with $maxLCBI_{4\ mm}$ greater than or equal to 600, which are regarded as having a high risk of PMI (13). Considering the results in the current study, this negative result could be attributed to a limited predictive capability of $maxLCBI_{4\ mm}$ at NIRS. Notably, this study found PMR, rather than $maxLCBI_{4\ mm}$, to be the most potent predictor of PMI. A neurointerventional study reported that the clinical outcome after mechanical thrombectomy depends on the predominant composition of the embolus (34). Therefore, the selection of optimal preventive strategies may differ based on the plaque composition: lipids, erythrocyte-derived materials, or a combination of both. MRI has the potential to provide new clues about preventive strategies for PMI.

This study had several potential limitations. First, the selection of intravascular imaging modalities was based on the operators' discretion, which could introduce selection bias. Second, due to the expected low mortality rate at 1 year in the present study involving a relatively small number of patients, we did not conduct an outcome analysis. Further investigation is necessary for a larger cohort of patients to determine whether the combination of NIRS and MRI offers additional prognostic information after PCI. Third, the relatively limited spatial resolution of MR images posed challenges for precise colocalization between MRI and NIRS-IVUS, thereby affecting their incremental predictive values. Finally, both 1.5-T and 3.0-T scanners were used, which may potentially affect PMR values. Due to the limited number of patients, especially those imaged with the 3.0-T scanner, subgroup analyses for each scanner were not feasible in this study.

In conclusion, erythrocyte-derived materials within coronary plaques, demonstrated with a high PMR value at T1-weighted MRI, were strongly associated with the development of PMI, independent of lipids. MRI may play a crucial role in predicting PMI by offering unique pathologic insights into plaques from a different perspective than lipid assessment with NIRS.

Author contributions: Guarantors of integrity of entire study, **H.M.**, **K.I.**, **S.H.**, **H.T.**, **Y.K.**, **R.K.**, **T.S.**; study concepts/study design or data acquisition or data analysis/interpretation, all authors; manuscript drafting or manuscript revision for important intellectual content, all authors; approval of final version of submitted manuscript, all authors; agrees to ensure any questions related to the work are appropriately resolved, all authors; literature research, **K.I.**, **H.M.**, **D.L.**, **D.D.**, **M.N.**, **R.K.**, **T.H.**, **Y.X.**, **T.S.**; clinical studies, **K.I.**, **H.M.**, **D.I.**, **H.T.**, **M.N.**, **H.O.**, **R.K.**, **T.H.**, **I.S.**, **T.S.**; statistical analysis, **K.I.**, **H.M.**, **D.D.**, **S.C.**, **S.H.**, **M.N.**, **R.K.**, **T.H.**, **T.S.**; and manuscript editing, **K.I.**, **H.M.**, **D.L.**, **P.J.S.**, **D.D.**, **S.H.**, **M.N.**, **R.K.**, **T.H.**, **A.G.C.**, **Y.X.**, **T.S.**

Disclosures of conflicts of interest: **K.I.** No relevant relationships. **H.M.** No relevant relationships. **D.L.** Grant from Siemens made to institution; honoraria and travel support from Siemens. **P.J.S.** Grants from the National Institutes of Health; software royalties from Cedars-Sinai Medical Center; consultant for Synektik SA. **D.D.** Software royalties from Cedars-Sinai Medical Center; associate editor for *Radiology: Cardiothoracic Imaging*. **S.C.** No relevant relationships. **D.I.**

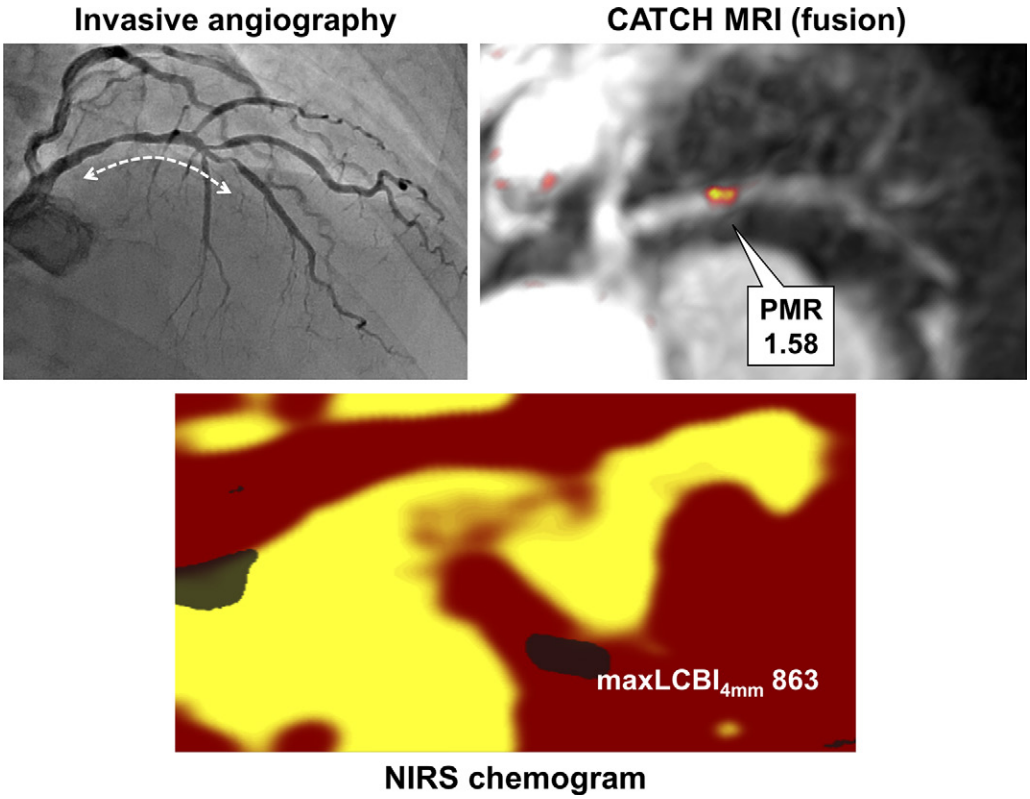

Figure 6: A representative case of a lesion associated with periprocedural myocardial injury. An example of a lesion with high-intensity plaque and lipid-rich plaque in a 49-year-old male patient is presented (the same patient as depicted in Figure 1). Invasive coronary angiographic image (upper left) shows moderate stenosis in the proximal segment of the left anterior descending coronary artery and severe stenosis in the midsegment. The treated segment at invasive coronary angiography is indicated by a dashed line. A fusion coronary atherosclerosis T1-weighted characterization (CATCH) MR image (upper right) exhibits a bright-blood anatomic reference with a color-coded overlay based on signal intensity at dark-blood T1-weighted imaging. High-intensity signals were observed in the proximal segment with a PMR value of 1.58, indicating the presence of high-intensity plaque. The NIRS chemogram (lower) corresponding to the treated segment is displayed. The distribution of lipid probability is quantitatively coded on a color scale from red (0) to yellow (1), calculated from the spectral data. The x-axis corresponds to pullback in millimeters, and the y-axis represents the circumferential position. The lipid core burden index is calculated as the proportion of pixels with a lipid plaque probability of 0.6, multiplied by 1000. Maximum 4-mm lipid core burden index (maxLCBI$_{4\ mm}$) represents the maximum value of lipid core burden index for a 4-mm-long segment. This lesion was classified as lipid-rich based on a maxLCBI$_{4\ mm}$ value of 863. NIRS = near-infrared spectroscopy, PMR = plaque-to-myocardium signal intensity ratio.

No relevant relationships. **S.H.** Unpaid academic editor for PLOS ONE. **H.T.** No relevant relationships. **M.N.** No relevant relationships. **Y.K.** No relevant relationships. **H.O.** No relevant relationships. **R.K.** No relevant relationships. **T.H.** No relevant relationships. **I.S.** No relevant relationships. **H.L.L.** No relevant relationships. **A.G.C.** Grants from the National Institutes of Health made to institution (grant nos. R01 HL156818, R01 EB028146, R01 HL127153, R01 EB032801); travel support from Siemens Healthineers; U.S. and PCT patents file by institution (U.S. patent nos. 10,436,871; 11,022,666; 17/245,342; 63/497,239) (PCT patent nos. PCT/US2019/051664; PCT/US2020/050247; PCT/US2021/30667; PCT/US2021/037695); executive board member of the Society for Magnetic Resonance Angiography. **Y.X.** No relevant relationships. **T.S.** No relevant relationships.

References

1. Zeitouni M, Silvain J, Guedeney P, et al; ACTION Study Group. Periprocedural myocardial infarction and injury in elective coronary stenting. Eur Heart J 2018;39(13):1100–1109.
2. Kimura S, Sugiyama T, Hishikari K, et al. Association of Intravascular Ultrasound- and Optical Coherence Tomography-Assessed Coronary Plaque Morphology With Periprocedural Myocardial Injury in Patients With Stable Angina Pectoris. Circ J 2015;79(9):1944–1953.
3. Silvain J, Zeitouni M, Paradies V, et al. Procedural myocardial injury, infarction and mortality in patients undergoing elective PCI: a pooled analysis of patient-level data. Eur Heart J 2021;42(4):323–334.
4. Bulluck H, Paradies V, Barbato E, et al. Prognostically relevant periprocedural myocardial injury and infarction associated with percutaneous coronary interventions: a Consensus Document of the ESC Working Group on Cellular Biology of the Heart and European Association of Percutaneous Cardiovascular Interventions (EAPCI). Eur Heart J 2021;42(27):2630–2642.
5. Brilakis ES, Abdel-Karim AR, Papayannis AC, et al. Embolic protection device utilization during stenting of native coronary artery lesions with large lipid core plaques as detected by near-infrared spectroscopy. Catheter Cardiovasc Interv 2012;80(7):1157–1162.
6. Sato A, Aonuma K. Coronary plaque morphology on multi-modality imaging and periprocedural myocardial infarction after percutaneous coronary intervention. Int J Cardiol Heart Vasc 2016;11:43–48.
7. Goldstein JA, Grines C, Fischell T, et al. Coronary embolization following balloon dilation of lipid-core plaques. JACC Cardiovasc Imaging 2009;2(12):1420–1424.
8. Goldstein JA. Peri-procedural myocardial infarction: Plaques and patients "at-risk". Catheter Cardiovasc Interv 2017;90(6):915–916.
9. Kuku KO, Singh M, Ozaki Y, et al. Near-Infrared Spectroscopy Intravascular Ultrasound Imaging: State of the Art. Front Cardiovasc Med 2020;7:107.
10. Goldstein JA, Maini B, Dixon SR, et al. Detection of lipid-core plaques by intracoronary near-infrared spectroscopy identifies high risk of periprocedural myocardial infarction. Circ Cardiovasc Interv 2011;4(5):429–437.
11. Kini AS, Motoyama S, Vengrenyuk Y, et al. Multimodality Intravascular Imaging to Predict Periprocedural Myocardial Infarction During Percutaneous Coronary Intervention. JACC Cardiovasc Interv 2015;8(7):937–945.
12. Matsuoka T, Kitahara H, Saito K, et al. Utility of near-infrared spectroscopy to detect the extent of lipid core plaque leading to periprocedural myocardial infarction. Catheter Cardiovasc Interv 2021;98(5):E695–E704.

13. Stone GW, Maehara A, Muller JE, et al; CANARY Investigators. Plaque Characterization to Inform the Prediction and Prevention of Periprocedural Myocardial Infarction During Percutaneous Coronary Intervention: The CANARY Trial (Coronary Assessment by Near-infrared of Atherosclerotic Rupture-prone Yellow). JACC Cardiovasc Interv 2015;8(7):927–936.
14. Irie D, Matsumoto H, Isodono K, et al. Complementary roles of near-infrared spectroscopy and intravascular ultrasound in the prediction of periprocedural myocardial injury. Can J Cardiol 2023;39(11):1502–1509.
15. Asaumi Y, Noguchi T, Morita Y, et al. High-Intensity Plaques on Noncontrast T1-Weighted Imaging as a Predictor of Periprocedural Myocardial Injury. JACC Cardiovasc Imaging 2015;8(6):741–743.
16. Hoshi T, Sato A, Akiyama D, et al. Coronary high-intensity plaque on T1-weighted magnetic resonance imaging and its association with myocardial injury after percutaneous coronary intervention. Eur Heart J 2015;36(29):1913–1922.
17. Usami K, Watabe H, Hoshi T, et al. Impact of coronary plaque characteristics on periprocedural myocardial injury in elective percutaneous coronary intervention. Eur Radiol 2023;33(5):3020–3028.
18. Saba L, Saam T, Jäger HR, et al. Imaging biomarkers of vulnerable carotid plaques for stroke risk prediction and their potential clinical implications. Lancet Neurol 2019;18(6):559–572.
19. Sato S, Matsumoto H, Li D, et al. Coronary High-Intensity Plaques at T1-weighted MRI in Stable Coronary Artery Disease: Comparison with Near-Infrared Spectroscopy Intravascular US. Radiology 2022;302(3):557–565.
20. Xie Y, Jin H, Zeng M, Li D. Coronary Artery Plaque Imaging. Curr Atheroscler Rep 2017;19(9):37.
21. Xie Y, Kim YJ, Pang J, et al. Coronary Atherosclerosis T_1-Weighed Characterization With Integrated Anatomical Reference: Comparison With High-Risk Plaque Features Detected by Invasive Coronary Imaging. JACC Cardiovasc Imaging 2017;10(6):637–648.
22. Saito Y, Kobayashi Y, Fujii K, et al. Clinical expert consensus document on intravascular ultrasound from the Japanese Association of Cardiovascular Intervention and Therapeutics (2021). Cardiovasc Interv Ther 2022;37(1):40–51. [Published correction appears in Cardiovasc Interv Ther 2022;37(1):52.]
23. Nakazawa M, Matsumoto H, Li D, et al. Rapid three-dimensional quantification of high-intensity plaques from coronary atherosclerosis T_1-weighted characterization to predict periprocedural myocardial injury. J Cardiovasc Magn Reson 2024;26(1):100999.
24. Noguchi T, Kawasaki T, Tanaka A, et al. High-intensity signals in coronary plaques on noncontrast T1-weighted magnetic resonance imaging as a novel determinant of coronary events. J Am Coll Cardiol 2014;63(10):989–999.
25. Tanisawa H, Matsumoto H, Cadet S, et al. Quantification of Low-Attenuation Plaque Burden from Coronary CT Angiography: A Head-to-Head Comparison with Near-Infrared Spectroscopy Intravascular US. Radiol Cardiothorac Imaging 2023;5(5):e230090.
26. DeLong ER, DeLong DM, Clarke-Pearson DL. Comparing the areas under two or more correlated receiver operating characteristic curves: a nonparametric approach. Biometrics 1988;44(3):837–845.
27. Kuroiwa Y, Uchida A, Yamashita A, et al. Coronary high-signal-intensity plaques on T_1-weighted magnetic resonance imaging reflect intraplaque hemorrhage. Cardiovasc Pathol 2019;40:24–31.
28. Uzu K, Kawakami R, Sawada T, et al. Histopathological Characterization of High-Intensity Signals in Coronary Plaques on Noncontrast T1-Weighted Magnetic Resonance Imaging. JACC Cardiovasc Imaging 2021;14(2):518–519.
29. Matsumoto H, Xie Y, Li D, Shinke T. Non-lipid-rich low attenuation plaque with intraplaque haemorrhage assessed by multimodality imaging: a case report. Eur Heart J Case Rep 2021;5(12):ytab460.
30. Stuber M. CATCH the Wave of Coronary Atherosclerotic Plaque MRI. Radiology 2022;302(3):566–567.
31. Knuuti J, Wijns W, Saraste A, et al; ESC Scientific Document Group. 2019 ESC Guidelines for the diagnosis and management of chronic coronary syndromes. Eur Heart J 2020;41(3):407–477.
32. Moss AJ, Williams MC, Newby DE, Nicol ED. The Updated NICE Guidelines: Cardiac CT as the First-Line Test for Coronary Artery Disease. Curr Cardiovasc Imaging Rep 2017;10(5):15.
33. Gulati M, Levy PD, Mukherjee D, et al. 2021 AHA/ACC/ASE/CHEST/SAEM/SCCT/SCMR Guideline for the Evaluation and Diagnosis of Chest Pain: Executive Summary: A Report of the American College of Cardiology/American Heart Association Joint Committee on Clinical Practice Guidelines. Circulation 2021;144(22):e368–e454.
34. Maekawa K, Shibata M, Nakajima H, et al. Erythrocyte-Rich Thrombus Is Associated with Reduced Number of Maneuvers and Procedure Time in Patients with Acute Ischemic Stroke Undergoing Mechanical Thrombectomy. Cerebrovasc Dis Extra 2018;8(1):39–49.